Supplementary material S4

In supplementary material 4, the results of the declustered samples with energy releases ≥ *M*5.5 with outliers in Regions A, B and C are presented. The same declustering method used in supplementary material 3, and the same two methods of using Dst and using Kp and F10.7 to eliminate the space weather effects were used. The results are shown in Figures S1—S12. Table S1 shows the parameters of the declustered samples, and Table S2 shows the minimum p, associated D, locations, and r for the results shown in Figures S1—S12.

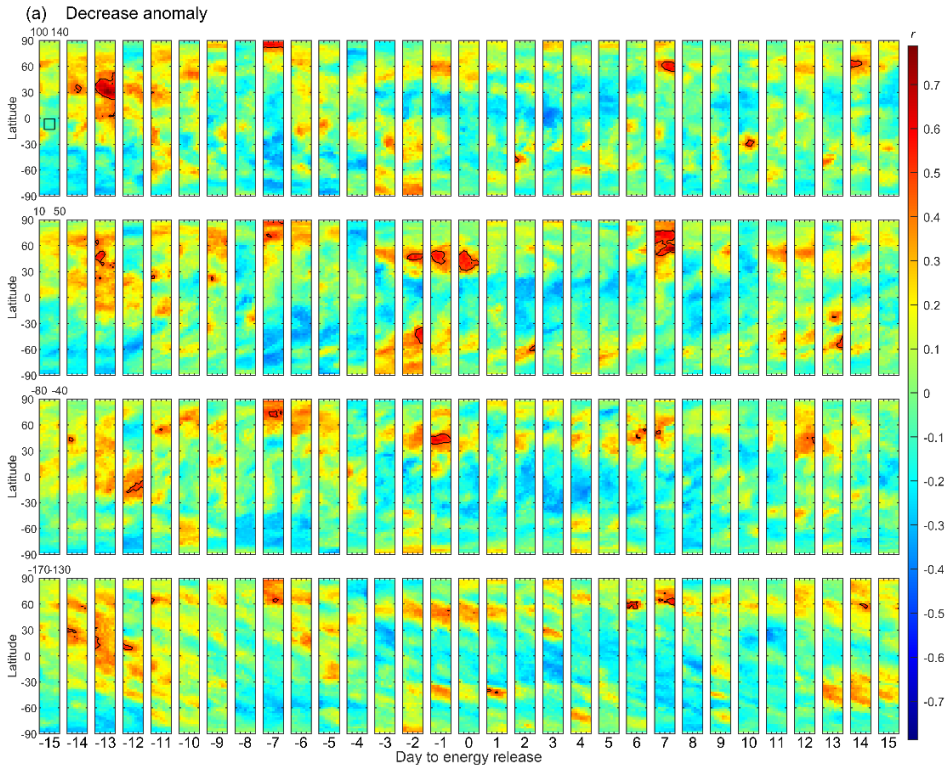

Figure S1. Distributions of the correlation coefficient of the TEC decrease anomaly for the declustered samples with energy releases ≥ *M*5.5 within Region A and with outliers. Data are removed using the Dst index.

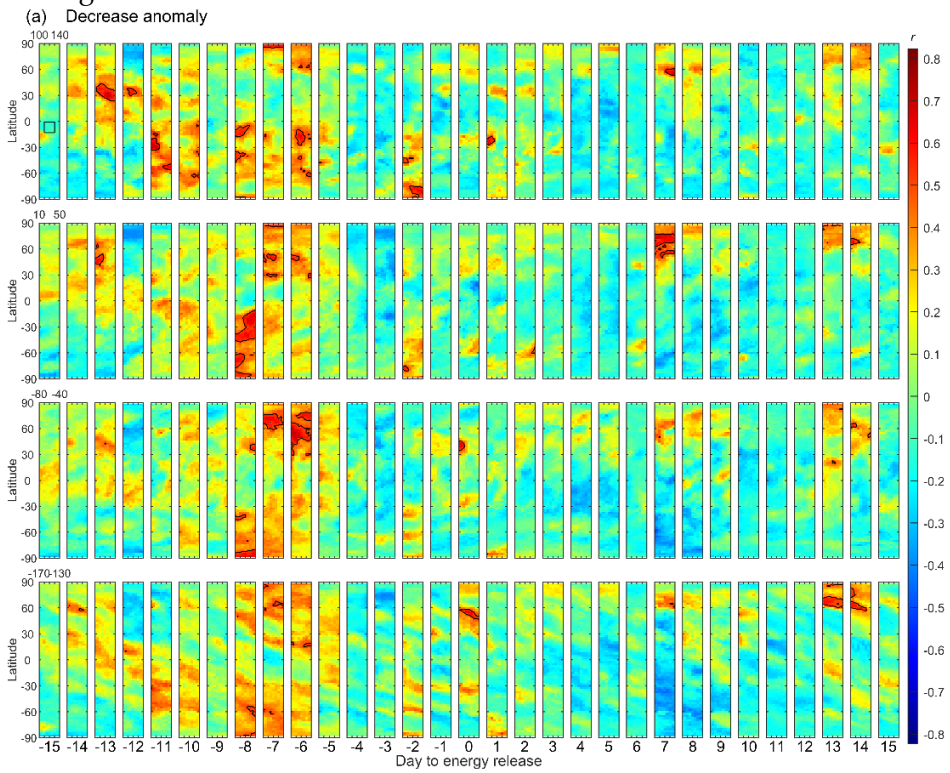

Figure S2. Same as Figure S1, but data are removed using Kp and F10.7.

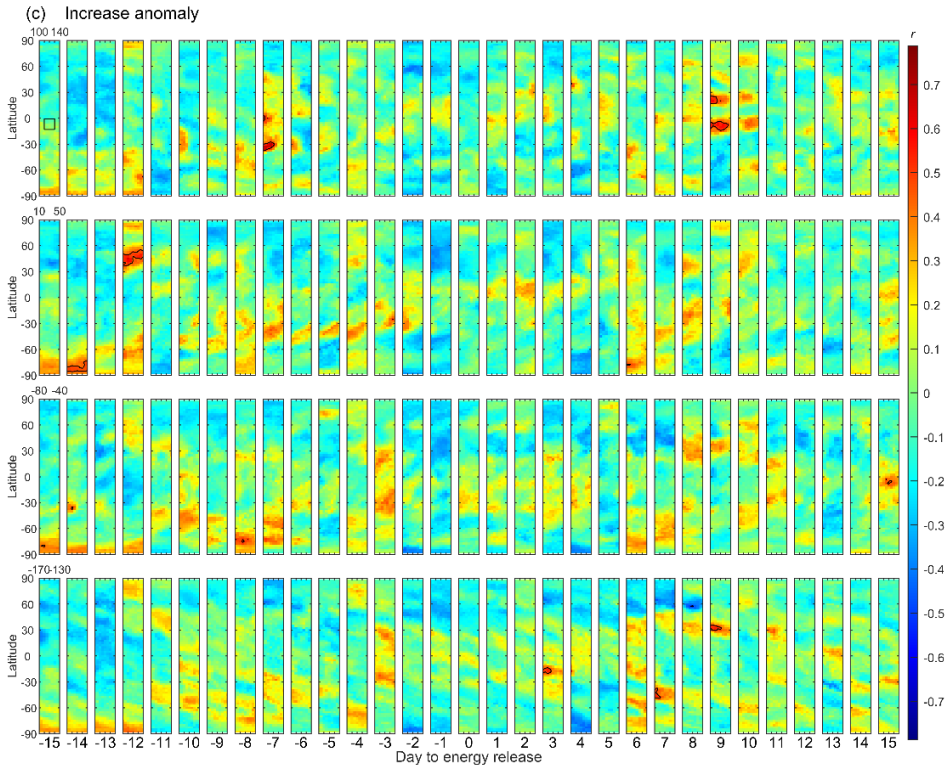

Figure S3. Distributions of the correlation coefficient of the TEC increase anomaly for the declustered samples with energy releases ≥ *M*5.5 within Region A and with outliers. Data are removed using the Dst index.

Figure S4. Same as Figure S3, but data are removed using Kp and F10.7.

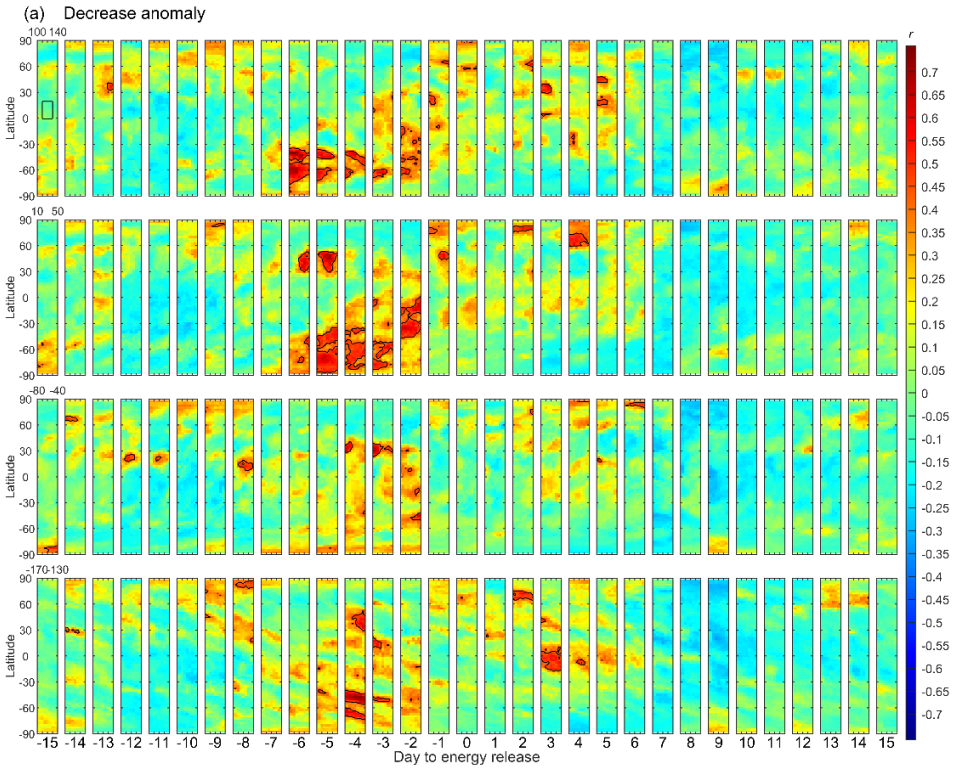

Figure S5. Distributions of the correlation coefficient of the TEC decrease anomaly for the declustered samples with energy releases ≥ *M*5.5 within Region B and with outliers. Data are removed using the Dst index.

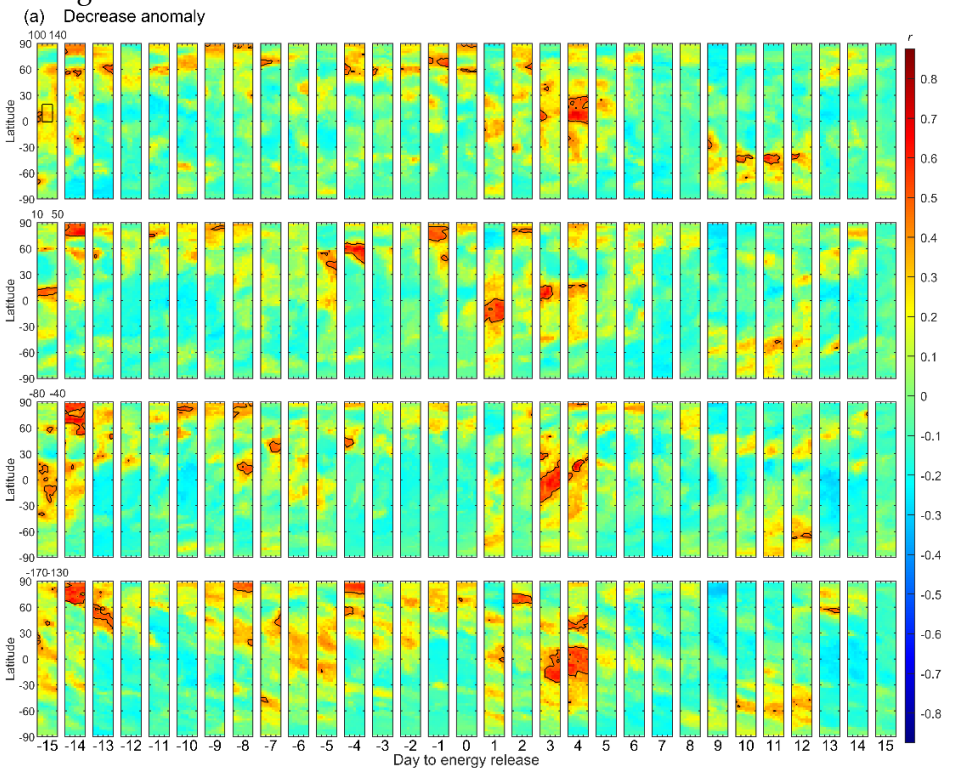

Figure S6. Same as Figure S5, but data are removed using Kp and F10.7.

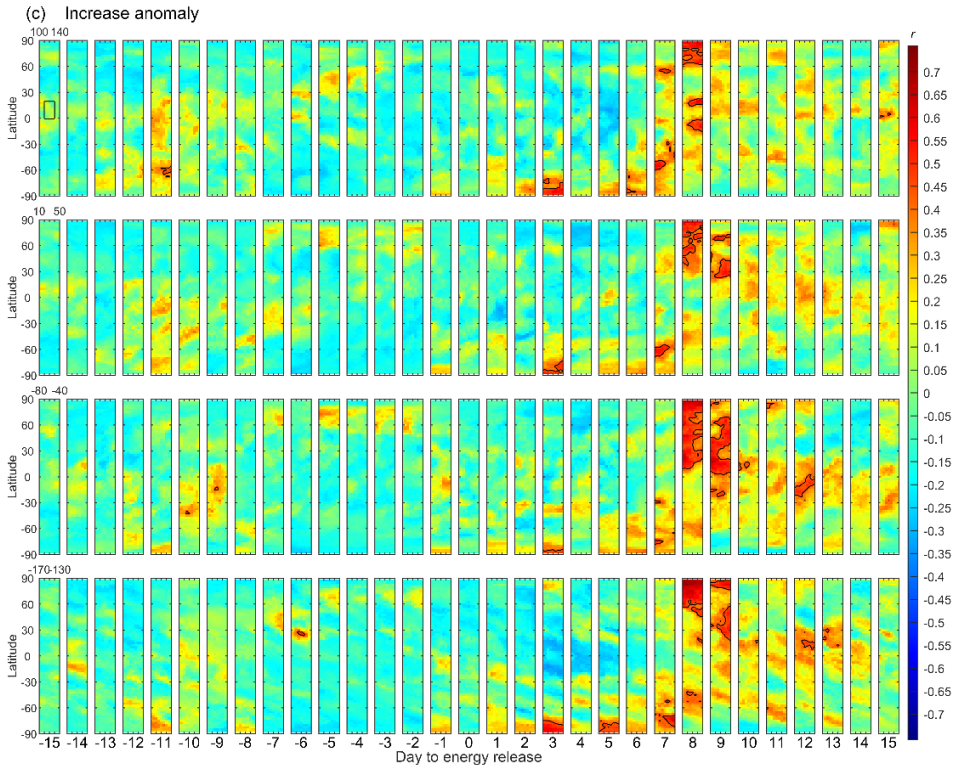

Figure S7. Distributions of the correlation coefficient of the TEC increase anomaly for the declustered samples with energy releases ≥ *M*5.5 within Region B and with outliers. Data are removed using the Dst index.

Figure S8. Same as Figure S7, but data are removed using Kp and F10.7.

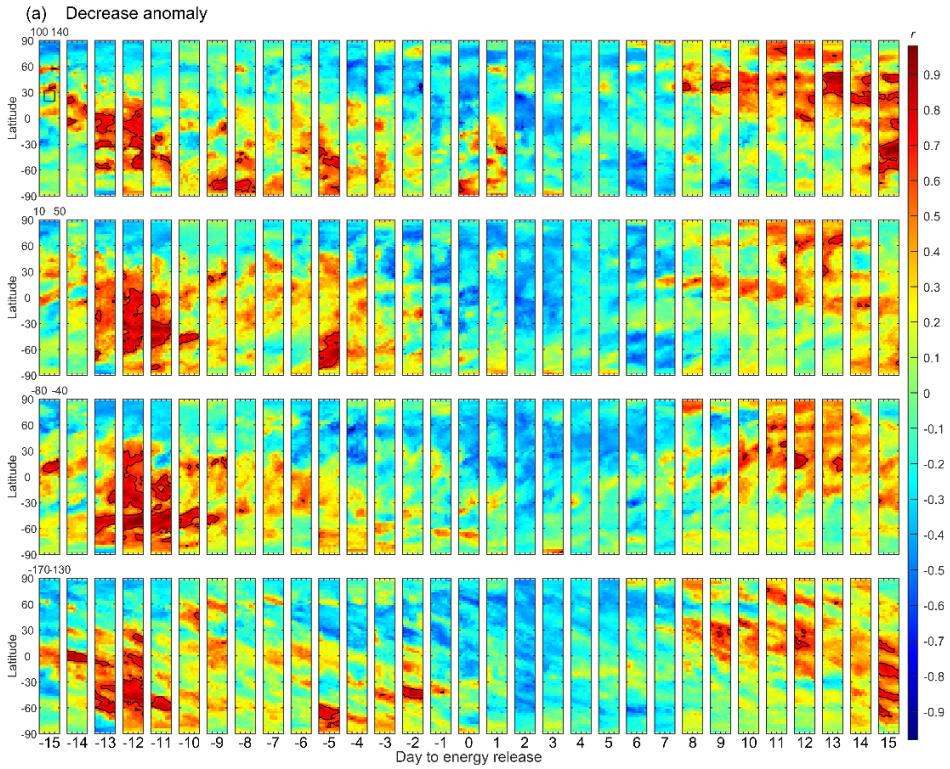

Figure S9. Distributions of the correlation coefficient of the TEC decrease anomaly for the declustered samples with energy releases ≥ *M*5.5 within Region C and with outliers. Data are removed using the Dst index.

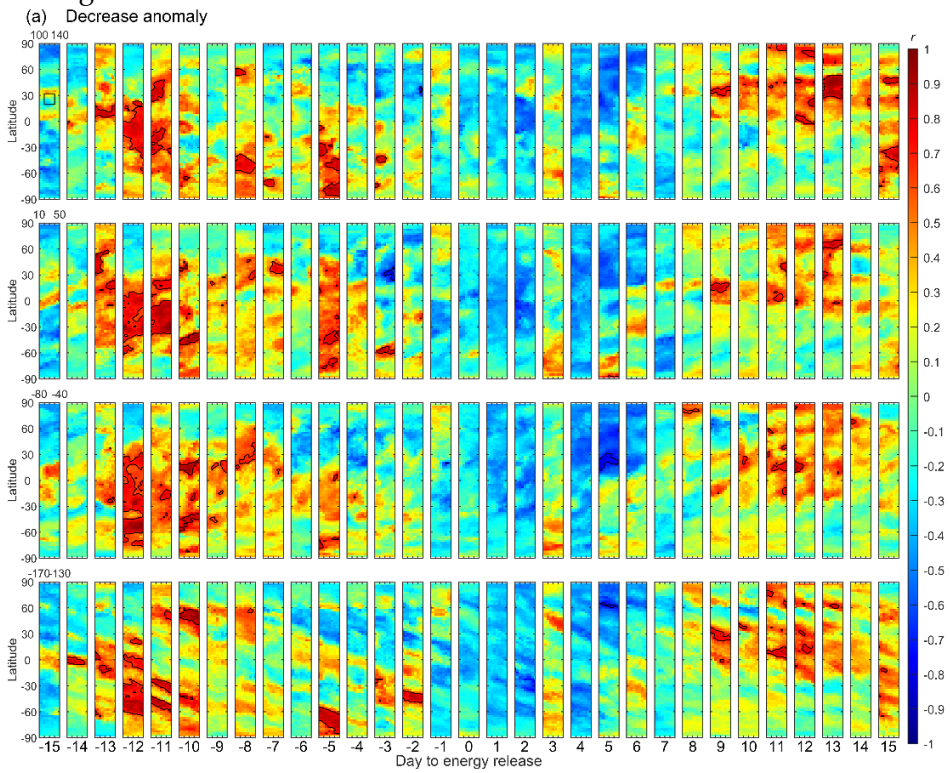

Figure S10. Same as Figure S9, but data are removed using Kp and F10.7.

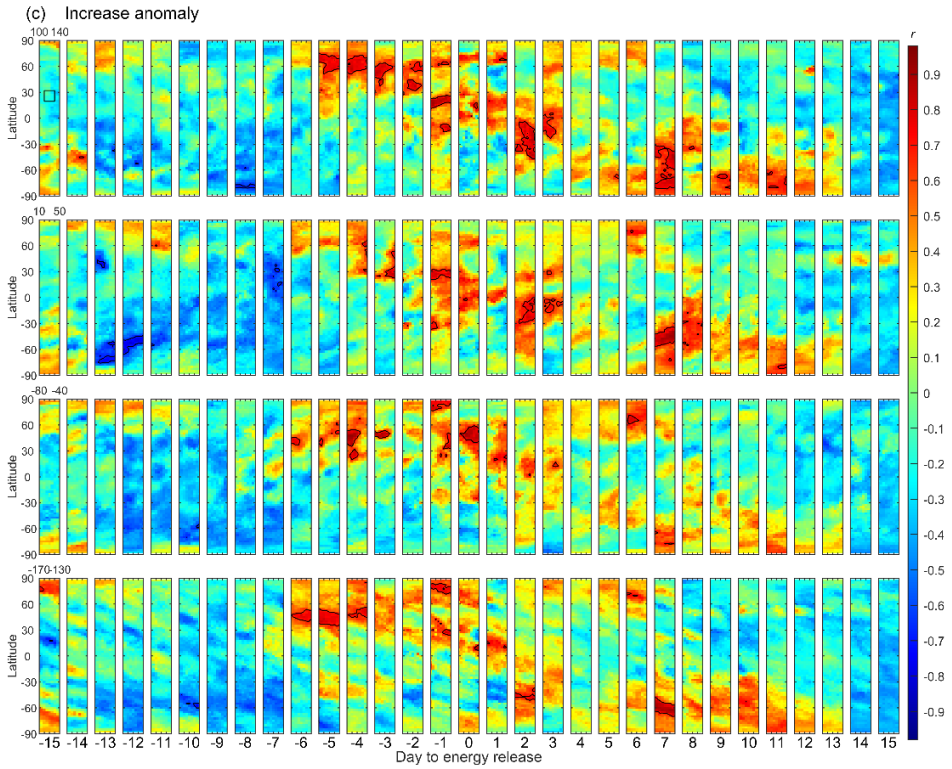

Figure S11. Distributions of the correlation coefficient of the TEC increase anomaly for the declustered samples with energy releases ≥ *M*5.5 within Region C and with outliers. Data are removed using the Dst index.

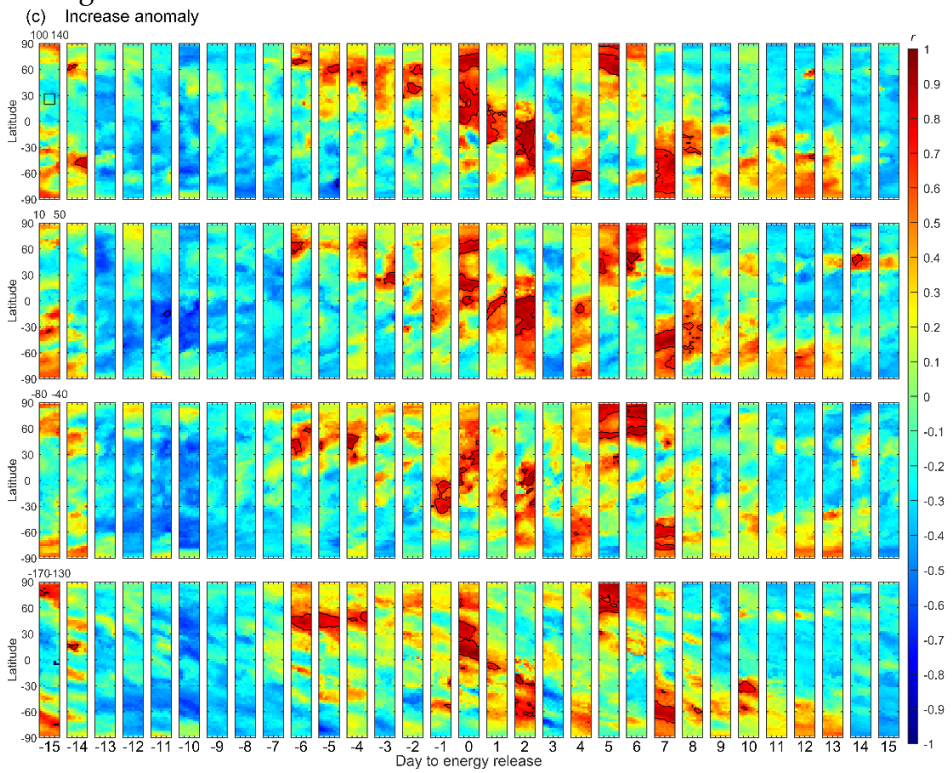

Figure S12. Same as Figure S11, but data are removed using Kp and F10.7.

Region	Using Dst			Using Kp, and F10.7		
	Sample size	$r_{\alpha=0.01}$	**Max. daily energy release in *M***	**Sample size**	$r_{\alpha=0.01}$	**Max. daily energy release in *M***
A	24－34	0.436－0.515	6.906－7.000	21－31	0.456－0.549	6.906－7.000
B	32－43	0.389－0.449	7.300－7.505	28－45	0.380－0.479	7.002－7.505
C	10－15	0.641－0.765	6.429－6.701	9－16	0.623－0.798	6.429－6.701

Table S1. Parameters for the declustered samples of daily energy release equivalent to *M* ≥ 5.5 earthquakes and with outliers. The left portion uses the Dst index, and the right portion uses Kp and F10.7 to eliminate the space weather effects.

			Min. *p*	D	Lat.	Long.	*r*
Region A	Using Dst index	Decrease anomaly	**1.598E-07**	**-13**	**32.5**	**125**	**0.783**
		Increase anomaly	6.166E-05	-7	-32.5	95	0.704*
	Using Kp and F107	Decrease anomaly	4.036E-06	-8	-17.5	65	0.756*
		Increase anomaly	7.127E-07	7	0	95	0.823*
Region B	Using Dst index	Decrease anomaly	1.792E-07	-4	-50	-130	0.756*
		Increase anomaly	2.243E-07	8	-10	155	0.744*
	Using Kp and F107	Decrease anomaly	1.842E-07	-4	60	35	0.706
		Increase anomaly	7.943E-14	13	7.5	-135	0.875*
Region C	Using Dst index	Decrease anomaly	4.196E-10	15	-35	125	0.980*
		Increase anomaly	1.525E-06	-4	47.5	-75	0.934
	Using Kp and F107	Decrease anomaly	3.849E-09	-11	-30	60	0.984
		Increase anomaly	7.780E-09	0	7.5	-145	0.988*

Table S2. The minimum *p*, associated D, locations, and *r* for the results shown in Figures S1－S12. The bold font denotes the minimum *p* that appears before energy release and in the 120 °E sector. The asterisk near *r* denotes that the associated *r* is the maximum *r* during D = -15 to 15 and over the 5,183 GIM grids.